Int. J. Therm. Sci. (1999) 38, 863–878

Numerical simulation of oscillatory Marangoni convective flow inside a cylindrical liquid zone

Hussein Bazzi[a], Cong Tam Nguyen[b], Nicolas Galanis[a*]

[a] *Department of Mechanical Engineering, Université de Sherbrooke, Sherbrooke (Québec), Canada J1K 2R1*
[b] *School of Engineering, Université de Moncton, Moncton (New Brunswick), E1A 3E9, Canada*

(Received 16 December 1998, accepted 24 March 1999)

Abstract — The problem of the oscillatory thermocapillary convection flow inside a $NaNO_3$ float zone which is suspended between a pair of coaxial disks with prescribed time-dependent temperature profiles and bounded by a cylindrical free surface, has been investigated. The system of governing equations corresponding to a three-dimensional transient model was directly solved by employing a finite control volume method, fully-implicit in time, and a staggered spatial mesh in cylindrical coordinates. It has been clearly shown that for a sufficiently low temperature difference between the disks, the flow consists of a steady and perfectly axisymmetrical toroidal structure with a purely axial movement of the fluid on the free surface and the vortex center located near that surface. Beyond the critical Marangoni number, $Ma_{cr}^{U} \approx 12\,500$, a transition from the axisymmetrical to the three-dimensional oscillatory state occurs. Under the effects of the time-dependent thermal disturbances on the free surface, the entire velocity and temperature fields rotate around the main axis following the second mode, i.e. the symmetrical mode of instability. A complete description of the flow structure and its dynamical behavior as well as a comparison with previous numerical and experimental data is given. The phenomenon of hysteresis has also been studied. It has been observed that there is a certain range of the Marangoni number where both the axisymmetrical and the oscillatory states may exist depending on whether the zone is heated up or cooled down. It has been found that the second critical Marangoni number i.e. the one corresponding to the reverse transition from the oscillatory to the axisymmetrical state, depends strongly on the temperature time-rate at which the zone is cooled. © 1999 Éditions scientifiques et médicales Elsevier SAS.

instability / thermocapillary flow / convection / float zone / microgravity / numerical simulation

Résumé — **Simulation numérique de l'écoulement thermocapillaire oscillatoire dans une zone liquide cylindrique.** On a étudié le problème de l'écoulement thermocapillaire oscillatoire à l'intérieur d'un pont liquide cylindrique de $NaNO_3$, suspendu entre deux disques coaxiaux dont les températures varient en fonction du temps. Le système des équations de conservation, correspondant à un modèle tridimensionnel en régime transitoire, a été résolu en utilisant la méthode des volumes finis. Cette méthode utilise un schéma totalement implicite dans le temps et un maillage décalé en coordonnées cylindriques. Il a été clairement montré que, pour un écart de température relativement faible entre les deux disques, l'écoulement est stationnaire et parfaitement axisymétrique, avec une structure unicellulaire dont le centre est localisé près de la surface libre. Au-delà du nombre de Marangoni critique, $Ma_{cr}^{U} \approx 12\,500$, la transition axisymétrique–oscillatoire a lieu. Sous l'effet de perturbations thermiques transitoires qui se propagent sur la surface libre, les champs thermique et hydrodynamique tournent autour de l'axe principal de la zone, en suivant le 2^{e} mode ou le mode symétrique de l'instabilité. Une description complète de la structure de l'écoulement et de son comportement dynamique, ainsi qu'une comparaison avec les données expérimentales, ont été établies. Le phénomène d'hystérésis a été également étudié. Il a été observé que, pour un certain domaine de valeurs du paramètre Ma, les états axisymétrique et oscillatoire peuvent exister, selon le type de transfert de chaleur, chauffage ou refroidissement, de la zone. Il a été également montré que le deuxième nombre de Marangoni critique correspondant à la transition inverse (oscillatoire–axisymétrique) dépend du taux temporel de refroidissement de la zone. © 1999 Éditions scientifiques et médicales Elsevier SAS.

instabilité / écoulement thermocapillaire / convection / pont-liquide / micro-gravité / simulation numérique

Nomenclature

A	aspect ratio, $A = R_0/H$	
C_p	specific heat of the fluid.....	$J{\cdot}kg^{-1}{\cdot}K^{-1}$
H	height of the float zone.....	m
k	thermal conductivity of the fluid...	$W{\cdot}m^{-1}{\cdot}K^{-1}$
Ma	Marangoni number, $Ma = \lvert\partial\sigma/\partial T\rvert\,\Delta T\,H/\mu\alpha$	
P	dimensionless pressure	

* Correspondence and reprints.

Pr	Prandtl number, $Pr = C_p\,\mu/k$	
R,θ,Z	dimensionless radial, tangential and axial coordinates	
R_0	radius of the zone	m
t,T	dimensional and dimensionless temperature	K
V_r	dimensionless radial velocity component	
V_θ	dimensionless tangential velocity component	
V_z	dimensionless axial velocity component	

Greek symbols

α	thermal diffusivity	$m^2 \cdot s^{-1}$
β	thermal expansion coefficient	K^{-1}
μ	dynamic viscosity	$kg \cdot m^{-1} \cdot s^{-1}$
ν	kinematic viscosity	$m^2 \cdot s^{-1}$
ρ	density	$kg \cdot m^{-3}$
σ	surface tension of liquid-vapor interface	$N \cdot m^{-1}$
τ	dimensional time	s
τ^*	dimensionless time	

1. INTRODUCTION

The float zone technique has become one of the most popular means to produce highly homogeneous and large crystals in space. Even under such strongly reduced gravity conditions, one must take into consideration the existence of the thermocapillary convection or the Marangoni flow which influences the entire domain. Its effects on the internal thermal field of a float zone have received considerable attention from many researchers, both experimentally (see, for example, [1–15]). A partial review of previous works in this area has been published by Wilcox [16].

Some observations performed in space and on earth-simulated-micro-gravity conditions have clearly shown that the steady axisymmetrical thermocapillary flow may become oscillatory and non-symmetrical when its intensity (which is proportional to the temperature gradient imposed along the free surface of the zone) is sufficiently vigorous. In fact, Preisser, Schwabe and Sharmann [3] have observed the oscillatory flow structure inside a tiny $NaNO_3$ float zone of ≈ 6 mm in diameter and ≈ 4 mm in height. Two different oscillatory modes were noticed: the first mode or the non-symmetrical mode which was detected for $R_0/H \leqslant 0.77$ and the second mode or the symmetrical mode which exists for $1.43 \geqslant R_0/H \geqslant 0.71$. For the first mode, the axis of the recirculation cell is inclined with respect to the zone centerline, and the whole field rotates around the latter. Several explanations for the instability mechanism have been proposed. Chun [2] and Preisser et al. [3], in particular, believed that the convection flow becomes unstable (i.e. oscillatory) when the Marangoni number which characterizes the intensity of the thermocapillary flow, exceeds a certain critical value Ma_{cr} ($Ma_{cr} \approx 10^4$ for $NaNO_3$). The critical Marangoni number likely remains constant for a given material in space and on earth and seems to be proportional to $Pr^{0.75}$. On the other hand, Vargas et al. [17] and Kamotaniet al. [18] have stipulated that the flexibility of the free surface itself may constitute a major factor in the generation of the oscillations. Ostrach et al. [4] have proposed an interesting physical model according to which the axisymmetrical/oscillatory transition is caused by a delay in the time-response between the thermocapillary flow near the surface and the return flow coming from the interior bulk fluid. Kamotani and Lee [19], from observations performed on Silicone oils, have suggested that the existence of a very thin thermal boundary-layer beneath the free surface may be a possible cause of the oscillations. The instability of the buoyant layers inside the float zone has been studied by Hu [6]. Also, according to Napolitano and Monti [20], the axisymmetrical/oscillatory transition occurs when the dynamic Weber number We_d — defined as the ratio of the dynamic pressure $\rho V^2/2$ and the rigidity due to the surface tension σ/H at the free surface – reaches a certain critical limit. They have proposed a new dimensionless parameter defined as $s = (2\,We_d)^{1/2}$ to characterize the onset of oscillations.

The experimental evidence of the existence of oscillations have initiated several analytical/numerical studies. Rupp et al. [21] simulated numerically an oscillatory flow within a half-zone of liquid GaAs. The agreement between their numerical results and experimental data can be qualified as acceptable, although relatively important errors were observed on the oscillations frequencies. Kazarinoff and Wilkowski [7, 22, 23] have numerically modeled a full-zone of Silicon, considering a deformable free surface but conserving, however, the axisymmetric character of the flow field. They have also investigated the oscillatory behavior of the flow. Direct numerical simulation has also been employed by Levenstam and Amberg [24] to study the stability of the flow in a half-zone of a small Prandtl number fluid, $Pr = 0.01$. The axisymmetric thermocapillary flow has been found to be unstable and turns into a steady non-axisymmetric state with azimuthal wave number equal to 2, for a zone aspect ratio of 1. With further increase of the thermocapillary Reynolds number, this steady three-dimensional solution loses its stability and becomes oscillatory. Both instabilities are believed to be hydrodynamic in nature. Recently, Savino and Monti [25] have studied the problem of the oscillatory Marangoni convection in a Silicone-oil liquid bridge ($Pr = 30$ and $Pr = 74$). They have shown that immediately after the onset of instability, the oscillatory flow can be described by a standing wave and a pulsating temperature distribution. When the oscillatory distur-

bances become large, the azimuthal velocity causes the rotation of "temperature-spots" along the free surface so that the time dependent temperature and velocity fields can be properly described by the dynamic model of an azimuthally traveling wave.

In spite of a considerable number of publications dealing with this problem, the physical mechanism that governs the onset of the time-dependent flow as well as the comprehensive picture of the flow organization remain, unfortunately, poorly understood. In the present paper, the problem of the hydrodynamic instabilities of the Marangoni flow inside a cylindrical float zone has been investigated by direct numerical simulation of a full three-dimensional and time-dependent model, considering $NaNO_3$ ($Pr = 8.9$) as the fluid and the micro-gravitational conditions. The objective of this work is not only to determine the critical Marangoni number, but also to provide complete information regarding the organization of the unstable flow structure as well as the effects due to the heating ramping-rate. We have also attempted to investigate the hysteresis phenomenon corresponding to the cooling process of the liquid zone, a phenomenon that has been observed experimentally.

2. MATHEMATICAL FORMULATION

2.1. Governing equations

We consider a cylindrical half-zone of a molten liquid which is held, under surface tension effects and micro-gravity conditions, between a pair of coaxial, parallel disks of radius R_0 and separated from each other by the distance H (*figure 1*). Both the disks are stationary and have uniform temperatures t_1 and t_2 ($t_1 > t_2$). In the present study, we will assign $t_2 = t_M$ where t_M is the melting temperature of the material considered, while the temperature $t_1 = f(\tau)$ varies as a function of time. For the proper mathematical formulation of the problem, the fluid is considered to be Newtonian and incompressible with constant properties evaluated at t_M, except for the surface tension which is acting on the zone free surface and assumed to be a linearly decreasing function of temperature:

$$\sigma = \sigma_M - \gamma (t - t_M) \tag{1}$$

The constant γ is assumed to be positive which means that the fluid particles will generally pull away from a high temperature spot on the free surface. The compression work, as well as the viscous dissipation, are considered to be negligible in the energy equation. Furthermore, the free surface of the zone is assumed thermally insulated and radially non-deformable, but can allow the transfer of heat and momentum in both

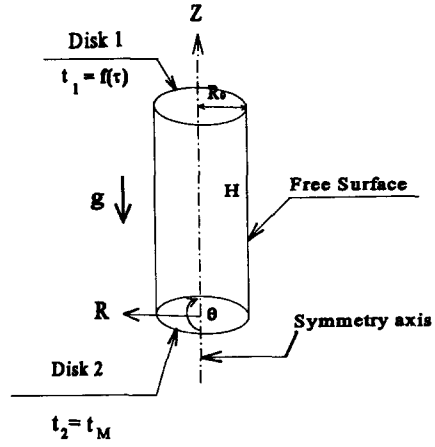

Figure 1. Geometry configuration of the thermocapillary flow.

the axial and circumferential directions. The assumption of a "thermally insulated" free surface was based on the fact that in real $\mu - g$ platforms, the float zone is generally well isolated from its surroundings, in order to ensure the uniformity of thermal boundary conditions as well as to keep the input power at a reasonably low level [26]. With regard to the assumption of the perfectly cylindrical shape of that surface, it is motivated by the fact that for the cases considered in this study, the capillary number, defined as $Ca = \gamma \Delta T / \sigma_M$, is very small ($\approx 10^{-3}$) indicating obviously the dominant effects of the surface tension (see in particular, Savino and Monti [25]). Furthermore, numerical simulations taking into account the deformability of the free surface have eloquently shown that under micro-gravity conditions (i.e. 10^{-4} g), the maximum radial deformation of that surface does not exceed, in any case, 0.08 % of the zone nominal radius [27].

The following quantities H, $(\gamma \Delta T/\mu)$, $(H\mu/\gamma \Delta T)$, $\rho(\gamma \Delta T/\mu)^2$, and $\Delta T = t_{1\,\mathrm{step}} - t_2$ have been respectively adopted as the reference length, velocity, time, pressure and temperature difference. Note that $t_{1\,\mathrm{step}}$ is the hot disk temperature corresponding to each of the heating steps considered, as shown later in *figure 2*. A dimensionless variable is then defined as the ratio of the quantity considered with respect to the corresponding reference quantity, except for the dimensionless temperature which is defined as follows:

$$T = \frac{t - t_2}{\Delta T} \tag{2}$$

Under the above conditions, the dimensionless governing equations written in the cylindrical coordinates system (R, θ, Z) are as follows [27]:

$$\nabla \cdot V = 0 \tag{3}$$

$$\frac{\partial V_i}{\partial \tau^*} + \nabla \cdot (V \cdot V_i) = -\nabla P + \frac{Pr}{Ma} (\nabla^2 V_i) + S_i \quad (i = 1, 2, 3) \tag{4}$$

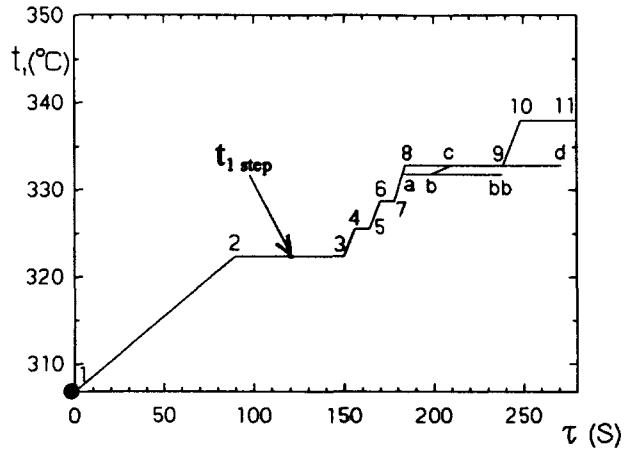

Figure 2. Time-variation of temperature as imposed on the disk No.1 during the heating process.

$$\frac{\partial T}{\partial \tau^*} + \nabla\cdot(\boldsymbol{V}\cdot T) = \frac{Pr}{Ma}(\nabla^2 T) \tag{5}$$

where $\boldsymbol{V} = (V_r, V_\theta, V_Z)$ is the velocity vector; τ^* is the non-dimensional time; S_1, S_2 and S_3 are the velocities-related stress terms given by:

- **for i = 1, the radial direction:**

$$S_1 = \frac{V_\theta^2}{R} - \frac{Pr}{Ma}\left(\frac{V_r}{R^2} + \frac{2}{R^2}\frac{\partial V_\theta}{\partial \theta}\right) \tag{6}$$

- **for i = 2, the circumferential direction:**

$$S_2 = \frac{Pr}{Ma}\left(\frac{2}{R^2}\frac{\partial V_r}{\partial \theta} - \frac{V_\theta}{R^2}\right) - \frac{V_r V_\theta}{R} \tag{7}$$

- **for i = 3, the axial direction:**

$$S_3 = 0 \tag{8}$$

and Ma and Pr are, respectively, the Marangoni number and the Prandtl number, given by:

$$Ma = \frac{\gamma\, \Delta T\, H}{\mu\, \alpha} \tag{9}$$

$$Pr = \frac{\nu}{\alpha} \tag{10}$$

The thermocapillary Reynolds number defined as $Re = Ma/Pr$ has often been introduced to characterize the circulation of the fluid due to the thermocapillary effect.

2.2 Boundary and initial conditions

The governing equations (3–5) constitute a set of non-linear and strongly coupled equations, and must be appropriately solved subject to the following boundary and initial conditions:

– on both disks, the usual non-slip and non-penetration conditions prevail; the disk No. 2 is held at constant temperature $T_2 = 0$, while T_1 varies with time τ^* according to an a priori known function (see for example, *figure 2*);

– the free surface, as stated previously, is considered thermally insulated and perfectly cylindrical; furthermore, the equations expressing the equilibrium of the shear stress in the axial and tangential directions must also be satisfied. The resulting boundary conditions are as follows: at $R = A = R_0/H$:

$$V_r = 0 \tag{11a}$$

$$\frac{\partial V_z}{\partial R} = -\frac{\partial T}{\partial Z} \tag{11b}$$

$$\frac{1}{A}\frac{\partial T}{\partial \theta} = -\left(\frac{\partial V_\theta}{\partial R} - \frac{V_\theta}{A}\right) \tag{11c}$$

$$\frac{\partial T}{\partial R} = 0 \tag{11d}$$

– as initial conditions, we assume that at the beginning of the heating process, i.e. at $\tau^* = 0$, the fluid is at rest and has a uniform temperature equal to its melting temperature t_M.

From the governing equations (3–5) and their boundary conditions, one can see that the problem under consideration is characterized by a set of three dimensionless parameters, namely the Marangoni number Ma, the Prandtl number Pr and the aspect ratio A.

3. NUMERICAL METHOD AND VALIDATION

The system of governing equations (3–5), subject to the specified boundary and initial conditions, has been successfully solved by employing the modified-SIMPLE method [28, 29]. In this method, which is based on the finite control volume approach, the governing equations are first integrated over a finite volume by assuming that heat, mass and momentum fluxes are uniform through any interface of the volume. The exponential scheme has been used throughout for the treatment of the combined convection and diffusion fluxes resulting from the transport process. For the transient problem which is under study here, the time-fully-implicit scheme has been employed throughout. Staggered grids have been used with the velocity components calculated at the six interfaces, while the pressure and other scalar quantities such as temperature and species concentration are computed at the center of the control-volume considered. The result of the

above integration process consists of a set of algebraic discretized equations which have been successfully solved by using the "line-by-line" technique with the aid of a standard TDMA (i.e. Three-Diagonal Matrix Algorithm). The numerical solution is sequential i.e one variable at a time. A special "pressure-correction" equation has been derived by a judicious combination of the discretized Navier-Stokes equations and the integrated continuity equation. This pressure-correction equation is then employed to determine the pressure field as well as to correct the velocities field in order to progressively, i.e. iteratively, satisfy all the discretized equations.

3.1. Grid and validation

In order to ensure the consistency as well as the precision of numerical results, several non-uniform grids have been submitted to a "two-part" testing procedure. First, with a fixed number of nodes along the θ-direction, we have simulated the particular case of the axisymmetrical thermocapillary convection in a $NaNO_3$ half-zone with $Ma = 10\,000$, $A = 0.732$ and $Pr = 8.9$ by varying the number of nodes in the radial and axial directions. Results in *table Ia* show that the grid $26(R) \times 26(Z)$ seems to be quite appropriate for the task demanded, since the relative error between grids does not exceed ≈ 4 %. In the second part of the testing, with this 26 × 26 grid in hand, the fully 3-D case of thermocapillary convection in a cylindrical half-zone ($Ma = 10\,000$, $A = 0.732$ and $Pr = 8.9$) has been carried out, by imposing "ad-hoc" non-symmetrical thermal boundary conditions. Results in *table Ib* confirm that 24 grid points in the θ-direction appear to be largely sufficient to ensure the precision of numerical results. Consequently, the $26(R) \times 26(Z) \times 24(\theta)$ non-uniform grid has been adopted for all the simulations performed in this study. Because of the high value of the Marangoni number considered for the above tests, we are quite confident that the chosen grid will be satisfactory for the entire range of Ma that will be studied in transient cases.

TABLE I
Results on different grids for $NaNO_3$.

(a) in the r–Z plane	
Grid $N_r \times N_z$	$V_{z\max}$ at free surface
24 × 24	0.082528
26 × 26	0.086641
28 × 28	0.090496
36 × 36	0.089304
42 × 40	0.090306
(b) In the θ direction	
26 (N_r) × 26 (N_z) × N_θ	$V_{z\max}$
20	0.026479
24	0.026288
28	0.026216

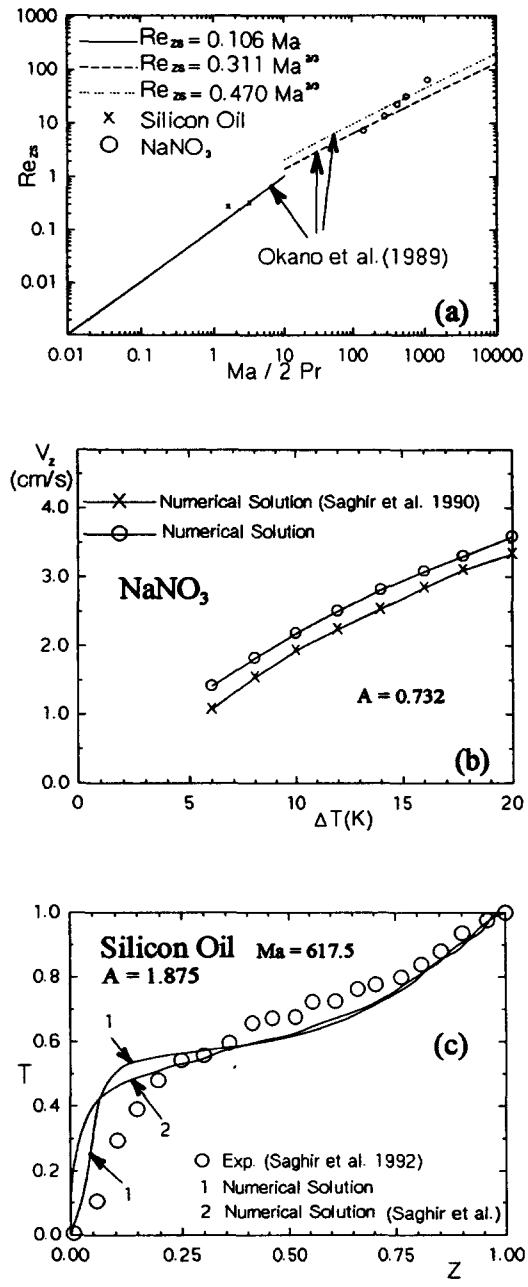

Figure 3. Comparison with other numerical and experimental data for **(a)**, **(b)** the fluid circulation on the free surface, and **(c)** the fluid temperature profile on the free surface.

The computer code was then extensively validated by comparing calculated results with available data in the literature. First, a comparison has been performed for the fluid axial velocity on the free surface with the corresponding empirical correlations by Okano et al. [30] (*figure 3a*), noting that the Reynolds number Re_{ZS} is defined as $Re_{ZS} = Ma\, V_{z\max}/2\, Pr$, where $V_{z\max}$ is the maximum fluid circulation on the free surface. The agreement can be qualified as quite acceptable. Good agreement has also been found between this maximum axial velocity obtained for $NaNO_3$ ($Pr = 8.9$) and the corresponding numerical results from a 2-D axisymmetrical model by Saghir and Rosenblat [31] (*figure 3b*). We have also attempted to validate the mathematical model under transient conditions. *Figure 3c* shows the comparison between numerical results obtained for a 2D-axisymmetrical half-zone of Silicone oil ($Pr = 196.5$) under transient regime/1-g conditions and the corresponding experimental data as well as numerical results by Saghir et al. [32]. Note that in this case, the deformable free surface has been taken into consideration. In spite of the experimental uncertainties regarding the measurement of temperature on the free surface, the agreement can be, once again, qualified as quite acceptable.

3.2. Other details regarding the numerical method

For all the numerical simulations performed in this work, a time step $\Delta\tau$ as small as 1/50 s has been employed while studying the oscillatory flow regime. At the beginning of the heating process, larger $\Delta\tau$, say $\Delta\tau = 1/20$ s, has been imposed in the time interval where no oscillations were expected. As convergence indicator at every time step, we used the "residual mass" which is resulting from the integration of the continuity equation (3) over a finite control-volume. Converged solutions were usually achieved with a very low value of this residual mass, i.e. a maximum of 0.001 % on the local basis. Under-relaxation factors ranging from 0.2 to 0.4 have been found to be quite appropriate, and no convergence difficulties have been experienced. In order to reduce the computing time while tracing the solutions corresponding to increasing values of the Marangoni number, an available converged solution obtained for a lower value of Ma was used as the initial conditions, and the flow has been simulated time-dependently until it has been judged to be either steady or periodic.

4. OSCILLATORY BEHAVIOR OF A MODERATE PRANDTL NUMBER FLUID ($NaNO_3$, $Pr = 8.9$)

The mathematical model as well as the computer code have been successfully validated and hence were used with confidence to study the transient behavior of a fluid zone. As a moderate Prandtl number fluid, $NaNO_3$ liquid with $Pr = 8.9$ has been selected because of available experimental data related to the axisymmetrical-oscillatory transition. *Figure 2* shows the time evolution imposed on the heated disk (i.e. disk no. 1) and *table II* summarizes details regarding the cases tested. Note that at the beginning of the heating process, i.e. at point 1 in *figure 2*, all the fluid zone is assumed to be at the melting temperature $t_M = 306.8$ °C.

TABLE II
Summary of cases simulated for $NaNO_3$ and heating disk No. 1 ($A = 0.732$) as specified in *figure 2*

Case	Temperature profile	$dt_1/d\tau$ (K·min^{-1})	Ma^*	Nature of the flow
I	(1, 2, 3)	10	7 500	axisymmetrical
II	(3, 4, 5)	30	9 000	axisymmetrical
III	(5, 6, 7)	30	10 500	axisymmetrical
IV	(7, 8, 9)	40	12 500	oscillatory
V	(9, 10, 11)	30	15 000	oscillatory
VI	(7a, b, bb)	40	12 000	axisymmetrical
VII	(b, c, d)	5	12 500	oscillatory

* Values of Ma correspond to ΔT of each step.

4.1. The basic state

The structure of the flow has been carefully scrutinized at regular intervals during the heating process, and this for all the cases considered. It has been clearly established that for the cases I, II, III and VI of *table II*, that is for $Ma \leqslant 12\,000$, the flow and the thermal fields remain perfectly steady and axisymmetrical (*figure 4*). The flow basic state consists of an usual toroidal structure with its vortex center located near the free surface close to the hot disk. One may notice the evident action of the thermocapillary effects on the free surface where a strong fluid circulation has been found. The return flow passes through the central region and carries lower temperature fluid away from the cold disk. The intensity of this thermocapillary-induced motion has been found to increase considerably with the increase of the Marangoni number. Such behavior is well known and consistent with experimental observations (see for example, Preisser et al. [3]). It is due to the fact that increasing Ma, or the temperature difference ΔT between the disks, results in an increase of the temperature gradient along the free surface and, consequently, to a corresponding increase of the thermocapillary flow . The basic state of the thermal field consists of perfectly circular and concentric isotherms in a plane normal to the main axis of the zone.

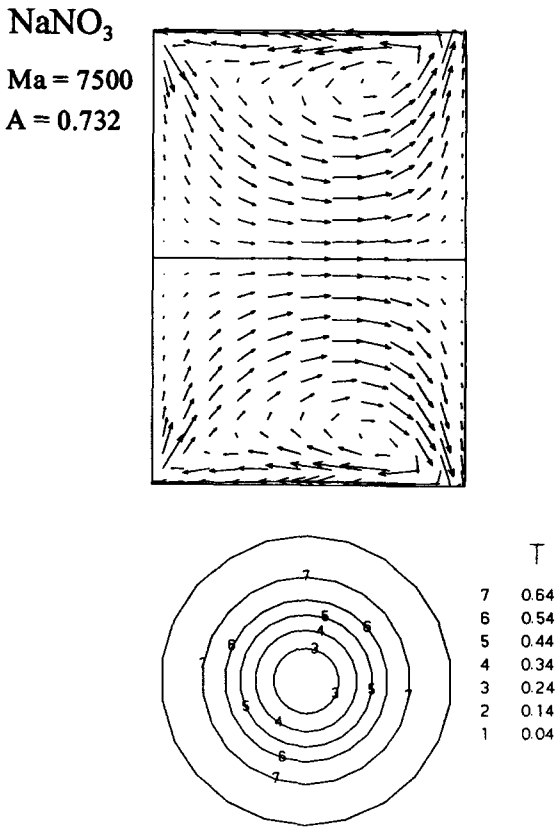

Figure 4. Axisymmetrical flow structure and thermal field ($NaNO_3$, $Ma = 7\,500$, $A = 0.732$).

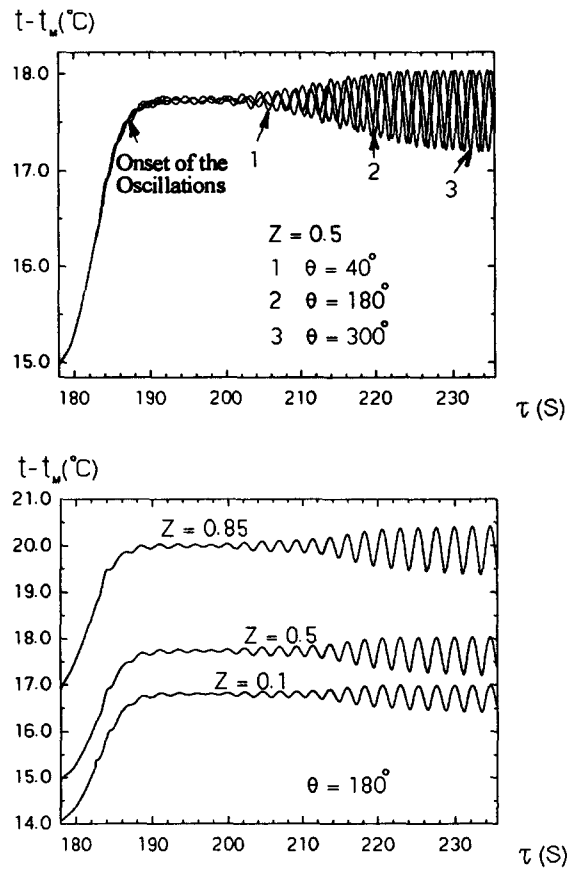

Figure 5. Time-evolution of fluid temperature for various particular points located on the free surface (case IV).

4.2. The transition to the oscillatory state

For sufficiently high Marangoni number, case IV with $Ma = 12\,500$ for example (*figure 5*), it is clearly established that the above steady axisymmetrical basic state is destroyed, and the flow gradually becomes three-dimensional and oscillatory with time. Note that the value $Ma = 12\,500$ is in fact the critical Marangoni number corresponding to that axisymmetrical/oscillatory transition. We will call it hereafter "the upper critical Marangoni number" or Ma_{cr}^{U}. For the case IV, shown in *figure 5*, one can observe that immediately after the onset of the oscillations, the amplitude of the oscillations remains relatively weak. In fact, except for the existence of a non-zero circumferential velocity component – in particular in the vicinity of the free surface – the loss of the flow symmetry remains almost imperceptible at this early stage. However, with further increase in time and under the constant value of ΔT imposed between disks, these oscillations grow steadily and become fully developed while perturbing considerably the entire flow field. One can notice the obviously unsteady and spatial character of these disturbances (*figure 5*). Thus, the temperature at a fixed point in space varies periodically with time around a certain average-value which is dictated by the local mean thermal field prevailing within the zone. As shown in subsequent sections, these temperature disturbances are also periodic with respect to the circumferential position. For instance, one may notice from *figure 5* that the amplitude of oscillations appears to be more pronounced near the heated disk. Thus, the peak-to-peak amplitude observed is approximately 0.57 K, 0.83 K and 1.03 K respectively for the planes $Z = 0.1$, 0.5 and 0.85. The frequency of the oscillations has been estimated to be $f_0 = 0.4$ Hz by using a FFT technique.

The above dynamical behaviors as well as the three-dimensional flow structure may be better understood by scrutinizing *figure 6* which shows the instantaneous flow pattern obtained for case IV in four particular R–Z planes. The coordinates of the vortex center have also been provided for discussion purpose. It is very interesting to observe that although the toroidal flow structure is still present, its vortex center as well as

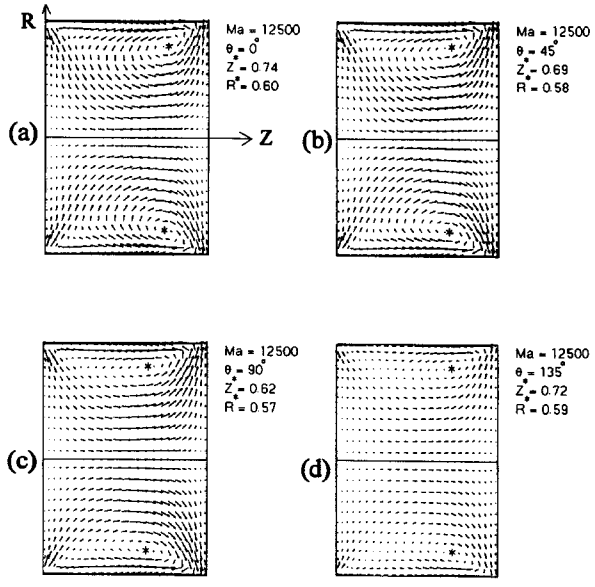

Figure 6. Instantaneous structure of the flow in four $R-Z$ planes for the case IV.

the velocity field in the bulk liquid zone change notably from one plane to another. In particular, the shift of the vortex center has been found to be quite appreciable along the axial direction. Thus, it is shifting from the position ($Z^* = 0.74$, $R^* = 0.60$) at the angular location $\theta = 0°$ to (0.69, 0.58), and (0.62, 0.57) and (0.72, 0.59) respectively for $\theta = 45°$, 90°, and 135°. The views for the angular locations $\theta = 0°$ (*figure 6a*) and $\theta = 90°$ (*figure 6c*) correspond approximately to the extreme positions of the vortex center. One can observe that associated with the above shift of the vortex center, the entire flow field also changes drastically with respect to the circumferential direction, in particular in the region beside the hot disk where the vortex center is confined. This explains the high amplitude of the fluid temperature oscillations observed in that region (see again, *figure 5*).

This striking 3-dimensional toroidal structure also changes periodically with time. *Figure 7* shows the instantaneous positions of the vortex center in the $R-\theta$ and $R-Z$ planes for two different instants τ and $\tau + \tau_0/2(\tau_0 = 1/f_0$ is the period of the oscillations). Although the variation in the position of the vortex center appears to be small for the fluid considered, these results illustrate eloquently the dynamic effects due to the oscillations on the flow field. One can see clearly from *figure 7c* that for a fixed time, the ring of vortex centers exhibits a symmetrical "saddle-like-shape", where its extreme shifts with respect to the axial direction may be noticed. In the $R-\theta$ plane, the projection of this vortex center ring follows a slightly elongated ellipse (*figure 7a*). This ring is also time-dependent as the entire temperature and velocity fields "rotate" around the circumference.

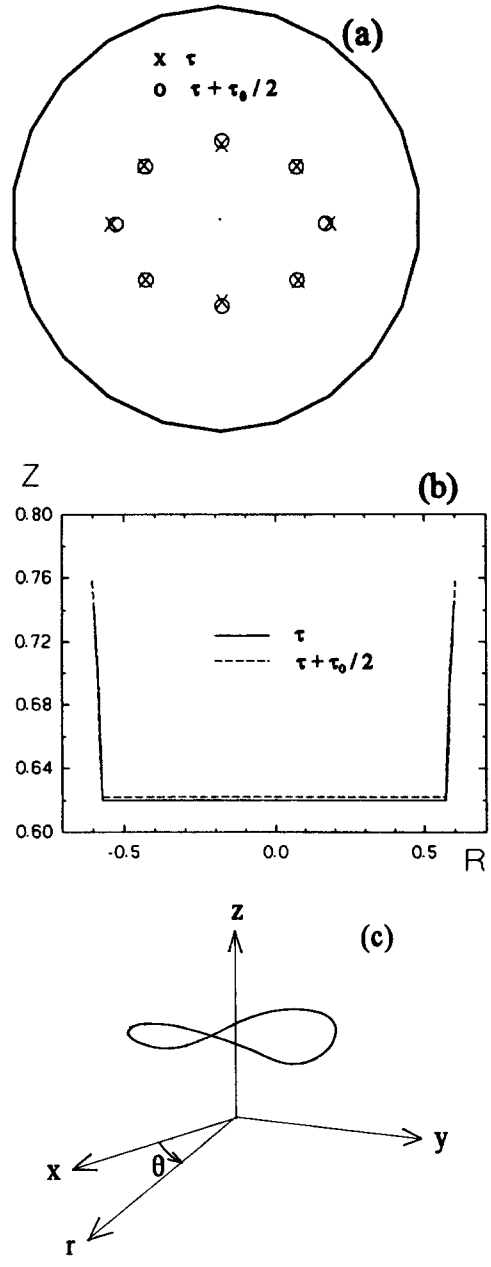

Figure 7. (a, b) Instantaneous positions of the vortex center for two different instants τ and $\tau + \tau_0/2$ (case IV), and (c) Illustrative view of the pathway of the vortex center (not to scale).

Figures 8 and *9* show respectively, instantaneous views of the velocity field and isotherms as obtained for the case IV at the cross-section $Z = 0.5$ (note that these views correspond in fact to four different instants τ, $\tau + \tau_0/4$, $\tau + \tau_0/2$ and $\tau + 3\tau_0/4$ during one oscillation cycle). We can obviously notice the rather complex behaviors of the flow and the thermal fields.

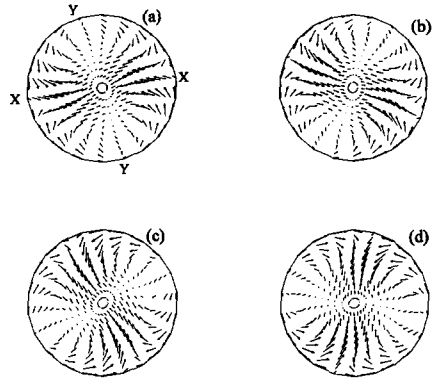

Figure 8. Instantaneous structure of the velocity field in the $r-\theta$ plane at $Z = 0.5$ (case IV) for four different times during one cycle.

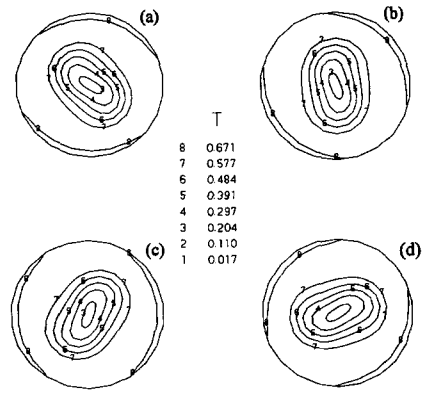

Figure 9. Instantaneous structure of the thermal field in the $r-\theta$ plane at $Z = 0.5$ (case IV) for four different times during one cycle.

Thus, for a fixed time, say at τ (*figures 8a* and *9a*), the transversal velocities are more pronounced in a large region around the line $X-X$ while along the line $Y-Y$, fluid circulation is drastically reduced. One may observe that in general, the fluid circulation on the free surface is more important. Furthermore, the region of high velocities i.e. the region along the axis $X-X$, is located at the junction of the two merging fluid streams moving radially away from the free surface. The coherent picture of the flow organization within the zone appears to be quite complex. It is observed that the fluid flow on the free surface is no longer purely axial, but clearly exhibits strong circumferential deviations. At the locations marked "Y", fluid coming axially from the hot disk splits into two streams while directing towards the cold disk. On the other hand, at locations marked "X", a merging of the two other deviated streams occurs. In the central region of the cross section, the return fluid from the cold end is also submitted to such circumferential deviation. With regard to the structure of isotherms in the $Z = 0.5$ plane, one can obviously observe that they are no longer circular as for the axisymmetrical case (see again, *figure 4*), but are now drastically distorted into an elongated shape which remains symmetrical with respect to the singular point. One may also notice the existence of the alternate hot and cold regions on the free surface. By scrutinizing *figures 8a* and *9a* for example, it can be observed that along the tangential direction on the free surface, fluid pulls away from a hot region and flows to the cold one, thus obeying to the well-known thermocapillary law. These alternate hot and cold regions, as well as the entire flow fields, exhibit a "rotating character" circumferentially around the main axis of the zone. Thus, the same flow and thermal fields are repeated exactly some time later at another angular position, creating the striking oscillatory effect in time as previously seen in *figure 5*.

The above detailed description of the flow field (see in particular, *figures 6* and *7*) indicates that we have present the second mode of instability according to the classification by Preisser et al. [3] and by Chun [33]. Note that this mode of instability, often referred as the "symmetrical mode", is characterized by a synchronous pulsation of a toroidal flow structure; while the first mode or the "asymmetrical mode" is represented by a rotating inclined torus with respect to the main axis. From observations performed on earth for $NaNO_3$, Preisser et al. [3] have found that the first and second modes exist, respectively, for $A \leqslant 0.77$ and $1.43 \geqslant A \geqslant 0.71$ (including transitional zones). The aspect ratio considered here, $A = 0.732$ falls within a transitional zone where both modes may exist as well.

In order to ascertain the oscillatory state observed in case IV as well as the value of the critical Marangoni number Ma_{cr}^{U} ($Ma_{cr}^{U} \approx 12\,500$ for the aspect ratio $A = 0.732$ considered here), the case VII has been simulated using as an initial conditions, the axisymmetrical flow field corresponding to the case $Ma = 12\,000$ (point b in *figure 2*), with a smoother temperature ramping-rate on disk No. 1, say $dt_1/d\tau = 5\ \mathrm{K \cdot min^{-1}}$. *Figure 10* shows the time-evolution of the temperature as obtained for the same point located on the free surface. It can be observed that the critical Marangoni number at which the transition to oscillations occurs does not seem to

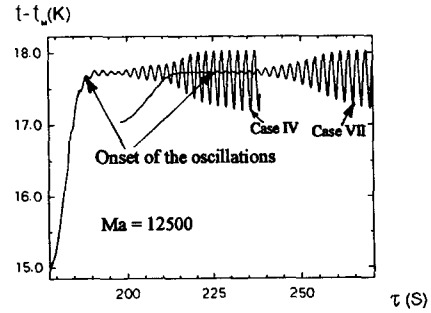

Figure 10. Time-evolution of the temperature of a particular point located on the free surface for cases IV and VII.

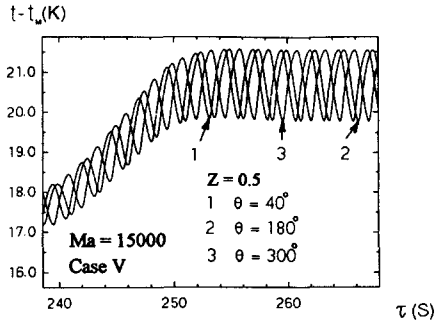

Figure 11. Time-evolution of the temperature of three particular points located on the free surface (case V).

vary with the values of $dt_1/d\tau$ imposed. For a lower ramping-rate as in case VII, only a small delay in time was detected for the onset of oscillations. Such behavior appears to be consistent with experimental observations by Schwabe and Scharmann [26, 34] as shown later in section 4.4. Also, the fully developed oscillatory flow structure, although being both time- and space-dependent, seems to have common characteristics which are proper to the level of the Marangoni number considered (for given values of Pr and A) and independent with respect to the time-history of the flow. Thus, for example, both temperature profiles shown in *figure 10* have identical frequency (0.4 Hz) as well as time-average value (324.53 °C) when the fully-developed oscillatory state is reached. The identical value of the averaged temperatures indicates eloquently that the "mean" flow, i.e. the one corresponding to the equilibrium state, is the same for the two cases considered, a fact which appears to be physically quite realistic. The deviations from that equilibrium state due to the instability may be different however, depending upon how the disturbances grow within the zone.

Finally, it has also been observed that for higher Marangoni numbers, say $Ma = 15\,000$ (case V), the effects due to the instability on the flow and thermal field become more pronounced. For example, the peak-to-peak amplitude of temperature oscillations for the three particular points on the free surface at $Z = 0.5$ is approximately 1.75 K under fully-developed oscillatory conditions (*figure 11*). It is very interesting to observe

TABLE III
Instantaneous positions of the vortex center in four different R–Z planes (case V).

θ	0°	45°	90°	135°
Z^*	0.77	0.73	0.62	0.59
R^*	0.61	0.59	0.57	0.58

the steady growth of the oscillations amplitude during the heating-up of the zone (note that the oscillations were already initiated within the zone since the initial conditions employed for case V correspond to the oscillatory state with $Ma = 12\,500$). Another point of particular interest resides in the fact that for case V ($Ma = 1\,000$), the effects of these oscillations on the flow and thermal fields are definitely more pronounced than those for case IV. Thus, one may observe from *figure 12a* that isotherms become considerably more distorted than those shown previously in *figure 9*. Also, the circumferential movement of the fluid in a $R-\theta$ plane is stronger, as it can be observed on *figure 12b* (note that the same scale was used for *figure 12b* and *figure 8*). The same behavior may also be noticed from the isotherms structure on the free surface (*figure 12c*) compared to that of the case $Ma = 12\,500$ (shown later on *figure 13*). *Table III* finally shows that for case V ($Ma = 15\,000$), the circumferential shift of the vortex center, in particular along the axial direction, appears to be more drastic in comparison with that for case IV (see again *figure 6*). From the above results, it can be deduced that the amplitude of oscillations as well as their effects on the flow and thermal fields become more important with higher Marangoni number. Such behavior, which is also consistent with that observed experimentally by Preisser et al. [3], will be better explained in the next section where the physical model governing these oscillations will be discussed.

4.3. On the cause of the oscillations

From the earlier description of the circumferential motion of the fluid on the free surface as well as

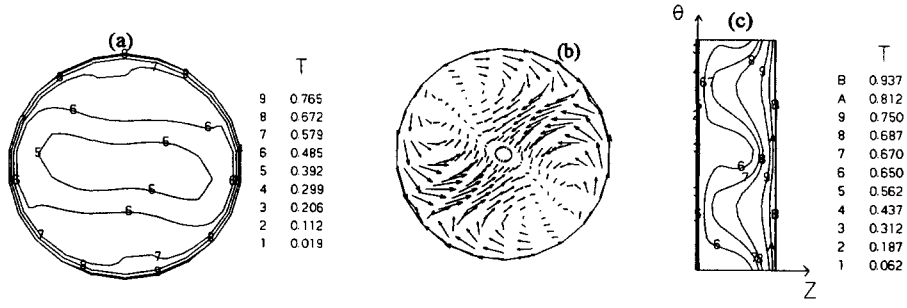

Figure 12. Instantaneous structure of (a) isotherms and (b) transversal velocity field in the middle plane $Z = 0.5$, and (c) isotherms on the free surface, for case V.

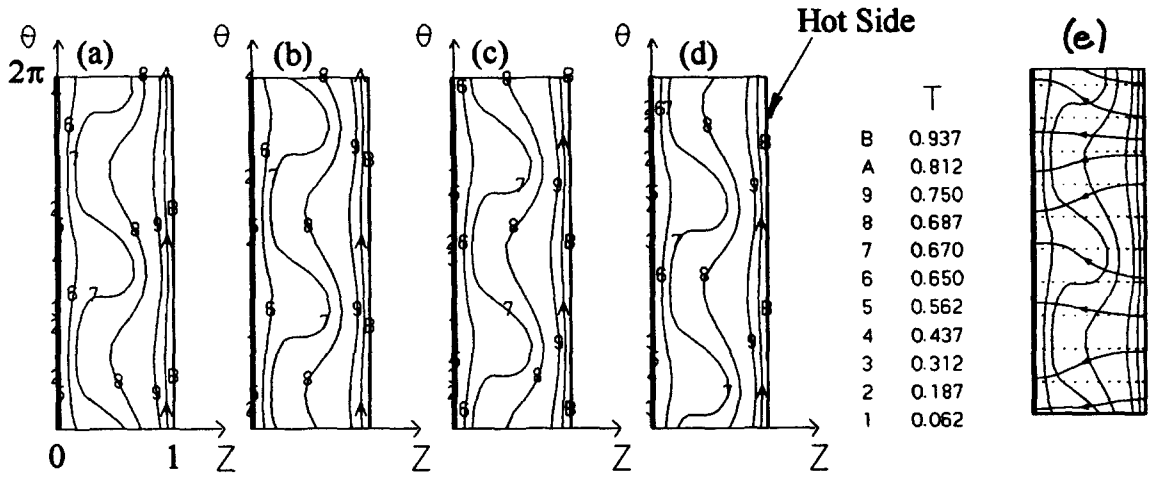

Figure 13. Instantaneous structure of (a–d) isotherms on the free surface for case IV at four different times during one cycle and (e) superposed isotherms and streamlines corresponding to frame "*a*".

the rotating and oscillatory behavior of the flow and the thermal field, and in conjunction with the striking similarity that exists between the time-variation of the fluid temperature (*figure 5*) and those observed by Preisser et al. [3], Savino and Monti [25] and also Schwabe and Scharmann [34], one can suggest that the observed oscillations are periodic in both space and time and of a thermal nature. Furthermore, these oscillations are believed to be the effects of the so-called "thermal traveling waves". In order to better explain this point, we have studied carefully the fluid thermal behavior on the free surface. *Figure 13(a–d)* shows the instantaneous snapshots of the isotherms structure on the free surface for the case IV ($Ma = 12\,500$) considered earlier. Note that these views correspond to four different times during one cycle. We can clearly observe that in the region close to the disks, the isotherms remain nearly parallel. However, in the large central region of the free surface, isotherms are drastically distorted into the form of a sinusoidal curve in the tangential direction, creating alternate hot and cold spots at any given axial position. This results in a non-zero temperature gradient along the circumference. Therefore, the thermocapillary surface flow is no longer "purely axial", but follows a curved pattern, as it can be clearly observed in *figure 13e* (this figure corresponds exactly to the same instant as that of frame "*a*"). We should note here that the fluid circulation on the free surface always obeys the thermocapillary law, i.e. fluid flows from a hot area towards a cold one. Furthermore, the periodicity both in space and time of the curved isotherms is clearly observed (*figure 13a–d*). As a result, the entire flow and thermal fields are dynamic and periodic in time. Thus, the above mentioned curved pattern of the fluid on the free surface also changes periodically with time, creating a rather complex flow structure in the bulk region (see again, *figures 6* and *8*). The flow is then associated with the corresponding rotation of the deformed torus around the main axis of the cylinder. It is very important to mention here that the instantaneous pattern of the isotherms and the streamlines shown in *figure 13e* is qualitatively quite similar to that observed experimentally by Schwabe and Scharmann [34] who, by careful measurements and observations performed on a NaNO3 float zone under normal gravity conditions, have clearly established the existence of the azimuthally traveling waves on the free surface of the liquid bridge.

As we have seen, the flow instabilities observed so far are likely to be caused by the existence of the periodic traveling thermal disturbances on the free surface. Such temperature disturbances lead to a continuous change of the temperature gradient along the circumferential direction and consequently, to a perturbation of the surface tension gradient. This results in some distortion of the velocity field which, in turn, is responsible for a drastic modification of the entire thermal field. Such a coupling between the surface tension effect and the heat transfer may lead to a growth or to a damping of the initial temperature disturbances. The formidable task is to determine the necessary conditions for which an amplification of an initial temperature disturbance would occur leading to a full establishment of the instability. According to Chun [2, 33] and Schwabe [1, 26, 34], the growth or the decay of a temperature disturbance on the free surface depends mainly on the relative importance between the thermocapillary convection effects and those of the diffusion i.e. on the order of magnitude of the Marangoni number itself. When the latter becomes sufficiently large, say $Ma \geqslant Ma_{cr}^{U} \approx 12\,500$ for the aspect ratio considered here, i.e. when the driving temperature difference exceeds a certain critical limit, an amplification of an initial temperature disturbance may occur since the beneficial damping effect due to the diffusion process (of heat and/or momentum) would become insufficient compared to the destabilizing effect caused by convection. Hence, the flow under a higher Marangoni

TABLE IV
Comparison with other experimental and numerical data for $NaNO_3$.

	(1)	(2)	(3)		(4)	(5)
	μ-g	μ-g	μ-g	1-g	μ-g	1-g
Ma_{cr}	12 500	11 633	9 444 ± 250	8 907 ± 150	≈ 9 000	≈ 8 000
Frequency (Hz)	0.4	0.56	0.48	0.51	0.5	0.57
$dt_1/d\tau$ K·min^{-1}	40.5	N/A	0.21	0.21	6	0.1

(1) Numerical results ($Pr = 8.9$)

(2) Numerical results from Rupp et al. [21].

(3) Experimental data from Schwabe and Scharmann [26].

(4) Experimental data ($Pr = 9.2$) from Schwabe and Scharman [34].

(5) Experimental data from Preisser, Schwabe and Scharmann [3].

N/A : not available.

number would, in general, be much more vulnerable with regard to the amplification of a disturbance. One can then expect that the effects due to the instability on the flow would become more important, as confirmed by the results for case V (*figures 11* and *12*). The above explanation regarding the onset of the oscillations based on the relative strength of the convection effects with respect to those of the diffusion process is somewhat analogue to that of the laminar/turbulent transition of a flow within a tube for which the forcing parameter is the flow Reynolds number.

4.4. Comparison with other experimental and numerical data

Table IV compares the critical Marangoni number and the oscillations frequency for $NaNO_3$ calculated in this paper with experimental and numerical data available in the literature. It is very interesting to observe that the frequency of the oscillations has been found to agree very well with the corresponding $\mu-g$ experimental data from Schwabe and Scharmann [26] as well as with numerical results from Rupp et al. [21]. One can notice however the notable difference between our values obtained for Ma_{cr}^{U} and those measured experimentally under $\mu-g$ environment. Such a difference may be attributed to several reasons. It should be noted, first, that there exists a major difference in the determination of the critical Marangoni number. In this study, Ma_{cr}^{U} corresponds in fact to the specific "steady-state" case where oscillations were detected through the tracing process. In various papers which reported experimental data related to the axisymmetric/oscillatory transition, such as those by Preisser et al. [3] and Schwabe and Scharmann [26], Ma_{cr}^{U} has been determined by employing a certain "extrapolation procedure" of the amplitude of oscillations with respect to the parameter Ma. Thus, the critical Marangoni number corresponds to a point where the amplitude is nearly zero. Also, it should be noted here that during these experiments, the amplitude of oscillations has been measured "unsteadily", i.e. while the heated disk temperature was on the rise. Secondly, in most cases, experimental operating conditions may not ensure totally the symmetric thermal boundary conditions. Therefore, the transition to a non-axisymmetrical time-dependent flow may occur at lower values of the Marangoni number, as noted by Rupp et al. [21]. Also, the properties of the melting substances used are, unfortunately, not known very accurately. The resulting discrepancy between the predicted and measured values of properties is often appreciable, ≈ 20 % according to the same authors. On the other hand, as stated previously, the presence of a deformable free surface may certainly create an aiding effect to the growth of a disturbance on that surface [4]. Such influence due to the deformation of the free surface may explain the lower critical Marangoni numbers generally observed on the Earth (*table IV*). Finally, with regard to the influence of the heating ramping-rate $dt_1/d\tau$ on the onset of the oscillations, it appears that the numerical results are also quite consistent with experimental observations. As stated previously, the occurrence of the axisymmetrical/oscillatory transition does not seem to vary significantly with respect to the value of $dt_1/d\tau$ imposed. This behavior can be confirmed by data from Schwabe and Scharmann [26, 34] shown in *table IV*, where relatively close values of the critical Marangoni numbers were obtained experimentally while using values of $dt_1/d\tau$ as different as 0.21 K·min^{-1} and 6 K·min^{-1}.

4.5. The transition from the oscillatory to the axisymmetrical state/the phenomenon of hysteresis

In the present work, we were also interested in studying the reverse trend, i.e. the transition from the oscillatory to the axisymmetrical state, which could occur normally during the cooling of the hot disk. Our study was mainly motivated by the existence of the hysteresis phenomenon associated with this reverse transition which has been observed experimentally by Schwabe and Scharmann [26] while working on a $NaNO_3$ float zone.

Figure 14 shows the two different time evolutions of the temperature $t_1(\tau)$ used for the cooling of the hot disk. Note that the same values of $|dt_1/d\tau|$ employed before for the heating process were imposed here. It is also important to mention that both temperature profiles begin at the same point "1", which corresponds in fact to the case $Ma = 12\,500$, $A = 0.732$. Calculations

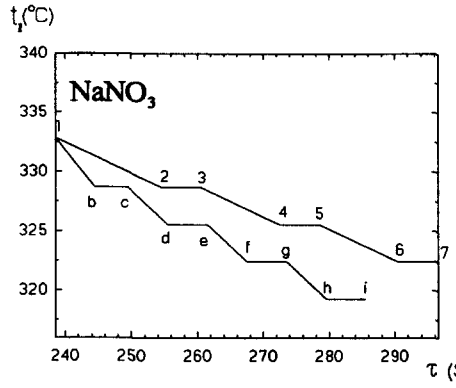

Figure 14. Temperature profiles of the disk no. 1 during the cooling process.

TABLE V
Summary of cases simulated for $NaNO_3$ and cooling disk no. 1 ($A = 0.732$) as specified in *figure 14*.

Case	Temperature profile	$dt_1/d\tau$ (K·min^{-1})	Ma^*	Nature of the flow
A	(1–2–3)	−15	10 500	Oscillatory
B	(3–4–5)	−15	9 000	Oscillatory
C	(5–6–7)	−15	7 500	Axisymmetrical
D	(1–b–c)	−40	10 500	Oscillatory
E	(c–d–e)	−30	9 000	Oscillatory
F	(e–f–g)	−30	7 500	Oscillatory
G	(g–h–i)	−30	6 000	Axisymmetrical

* Values of Ma correspond to ΔT of each step

TABLE VI
Peak-to-peak amplitude for $NaNO_3$ and two different ways of cooling disk No. 1.

Initial conditions Peak-to-peak amplitude = 0.83 K				$Ma = 12\,500$
Case	Peak-to-peak amplitude (K)		Case	Ma
A	0.52	0.45	D	10 500
B	0.10	0.26	E	9 000
C	Axisym. ≈ 0	0.11	F	7 500
		Axisym. ≈ 0	G	6 000

starting from this point, used as initial conditions the fully-developed oscillatory flow and thermal fields described earlier. The structure of the flow as well as the time-evolution of temperature were carefully traced and scrutinized for each of the cases tested. *Table V* summarizes the cases tested and traced and the nature of the flow as observed for these cases.

Figures 15 and *16* show the time-evolution of the fluid temperature for three particular points located on the free surface and at $Z = 0.5$, respectively, as obtained for the cases A, B and C (cooling pattern no. 1, $dt_1/d\tau = -15$ K/min) and the cases D, E, F and G (cooling pattern No. 2, $dt_1/d\tau = -30$ K·min^{-1}). It can be observed that with the decrease of the temperature difference ΔT between the disks, the amplitude of oscillations decreases progressively. For example, the peak-to-peak amplitude in K has decreased from 0.83 to 0.52 and to 0.10 approximately for Ma decreasing from 12 500 to 10 500, and to 9 000 while following the cooling pattern No. 1. On the other hand, the amplitude is respectively, 0.83 K, 0.45 K and 0.26 K for the same values of Ma on the cooling pattern No. 2. Note that the oscillations frequency is always the same: $f_0 = 0.4$ Hz for the aspect ratio $A = 0.732$ considered here. At sufficiently low value of ΔT or Ma, the temperature oscillations vanish completely and the flow becomes, again, perfectly axisymmetrical which can be detected when the three temperature profiles become identical. It is very interesting to observe that this second critical Marangoni number – hereafter called "the lower critical Marangoni number" or Ma_{cr}^{L} – corresponding to the oscillatory/axisymmetrical transition, is very different from one cooling pattern to another. Thus, the oscillatory state does no longer exists for the case C with $Ma = Ma_{cr}^{L} = 7\,500$ on pattern No. 1 while it still clearly persists for case F with the same value of Ma on pattern No. 2. In fact, with the second cooling pattern, a completely axisymmetrical flow structure has only been restored at $Ma = Ma_{cr}^{L} = 6\,000$. Hence, the hysteresis phenomenon clearly exists within the range $Ma_{cr}^{U} \geqslant Ma \geqslant Ma_{cr}^{L}$, where both the oscillatory and axisymmetrical states may exist depending whether we

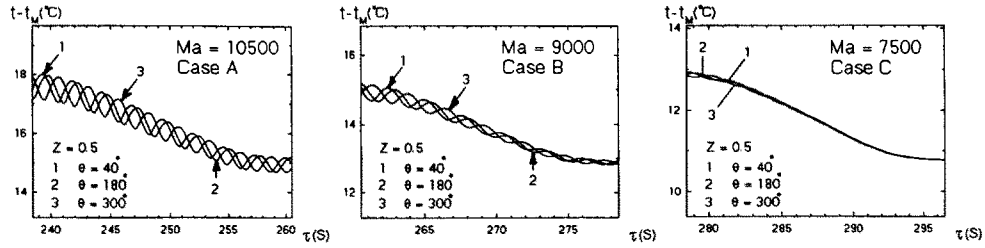

Figure 15. Time-variation of temperature at three particular points located on the free surface (cases A, B and C).

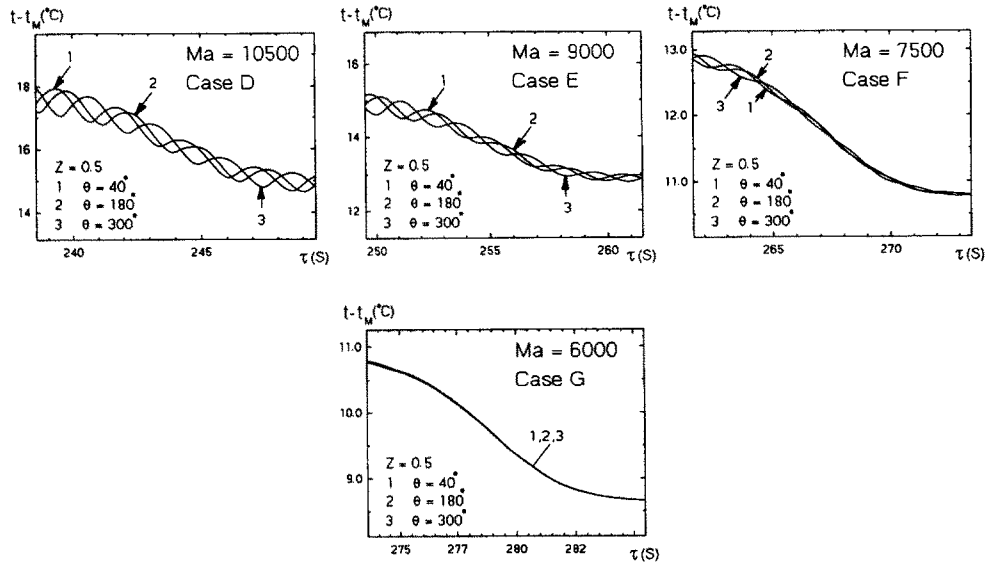

Figure 16. Time-variation of temperature at three particular points located on the free surface (cases D, E, F and G).

heat or cool the disk No. 1. This numerical prediction of the hysteresis phenomenon, which is believed to be the first of its kind, has been found to be quite consistent with the only available experimental observations by Schwabe and Scharmann [26]. The following comparison can be made, regarding the range of Ma where the hysteresis phenomenon is expected to occur:

Experimental data from Schwabe and Scharmann [26] give:

$9\,444 \geqslant Ma \geqslant 8\,340$, with $\mathrm{d}t_1/\mathrm{d}\tau = -0.43\ \mathrm{K{\cdot}min^{-1}}$

Present numerical study:

$12\,500 \geqslant Ma \geqslant 7\,500$, with $\mathrm{d}t_1/\mathrm{d}\tau = -15\ \mathrm{K{\cdot}min^{-1}}$

$12\,500 \geqslant Ma \geqslant 6\,000$, with $\mathrm{d}t_1/\mathrm{d}\tau = -30\ \mathrm{K{\cdot}min^{-1}}$

The agreement regarding the values obtained for the lower critical Marangoni number Ma_{cr}^{L} can be qualified as very good. Based on the trend of the numerical values for Ma_{cr}^{L} as function of $\mathrm{d}t_1/\mathrm{d}\tau$, it can be expected that for further decrease of the latter, the corresponding value of Ma_{cr}^{L} would approach 8 340, the value determined experimentally.

At this stage, two crucial questions of fundamental interest in fluid mechanics must be addressed. The first question concerns the phenomenon of hysteresis itself, and the second one is related to the existence of multiple lower critical Marangoni numbers associated with the oscillatory/axisymmetrical transition.

The fascinating phenomenon of hysteresis observed here may be explained primarily by the inertia effect of the liquid zone. This effect, present in the transfer of both heat and momentum, results in a lag in the response-time of the thermal and velocity fields corresponding to a change in the thermal boundary conditions imposed on the zone. On the other hand, the non- linear nature of the coupling between temperature and velocities also contributes to a rather complex and dynamical variation of the thermocapillary convection effects as well as those of the diffusion. The combination of these effects can affect greatly the growth or the decay of the thermal disturbances responsible of the oscillatory state. It should be noted that any decrease of the driving-temperature-gradient along the axial direction will eventually lead to an elimination of the thermal oscillations on the free surface and, hence, to a complete restoration of the axisymmetric base-state. Such behavior can be explained by the increase of the

stabilizing effects due to viscosity relatively to those of the thermocapillary convection, contrarily to the trend observed previously during the heating-up process where the drastic increase of the convection effects tends to destabilize the flow. This ratio of the relative strength between the convection and the diffusion effects appears, however, more complicated during the cooling process in the presence of an oscillatory flow within the zone. In fact, for a given value of ΔT or Ma, it is observed that oscillations decay more slowly with a higher ramp-rate $|dt_1/d\tau|$. Such a behavior, which appears somewhat paradoxical, may be explained by the fact that a rapid reduction of ΔT means that less time is allowed (to reach the same level of Ma) for the viscosity effects to overcome the perturbations due to the already existing oscillations. Time is therefore one of the crucial factors that governs the re-establishment of the axisymmetrical flow. The above behavior also explains the existence of the multiple values for Ma_{cr}^{L} obtained in this study.

5. CONCLUSION

In the present paper, the problem of the transition from the axisymmetrical to the oscillatory flow which occurs inside a $NaNO_3$ floating zone has been studied. An appropriate numerical model has been developed which allows a direct 3-D and time-dependent simulation of the hydrodynamic and thermal fields within the zone operating under $\mu - g$ conditions. The structure and the nature of the flow were carefully scrutinized at each of the stages during the heating process. The numerical results have revealed interesting behaviors which can be summarized as follows:

- under sufficiently low temperature differences between the disks i.e. low Ma, say $Ma < Ma_{cr}^{U} \approx 12\,500$, the flow remains perfectly steady and axisymmetrical and consists of a symmetrical torus with its vortex center located near the free surface of the zone;

- when the Marangoni number increases beyond Ma_{cr}^{U}, the transition from the above basic state to the oscillatory state occurs;

- the critical Marangoni number Ma_{cr}^{U} appears to be insensitive with respect to the ramping-rates tested;

- the oscillatory flow structure consists of a rather complex pattern with alternate hot and cold zones, and high and low velocity gradient regions on the free surface; the vortex center moves periodically along the radial and axial directions as the entire flow and temperature fields are rotating around the main axis of the zone;

- it appears that the instability, which is believed to be caused by azimuthally traveling thermal waves on the liquid free surface, is of the second mode i.e. the symmetrical mode.

The phenomenon of hysteresis has also been studied by comparing the transient behaviors of the zone during the heating and the cooling process. The following conclusions seem to be pertinent:

- there is a certain interval of Ma, say $Ma_{cr}^{U} > Ma > Ma_{cr}^{L}$, for which both oscillatory and axisymmetrical states may exist depending whether the zone is cooled or heated;

- the lower critical Marangoni number Ma_{cr}^{L} is not unique and strongly depends on the cooling ramping-rate imposed;

- the value of Ma_{cr}^{L} has been found to increase with decreasing cooling ramping-rate;

- the value of Ma_{cr}^{L} is expected to be within the interval (6 000, 7 500), based on the cases tested in this study.

Acknowledgements

The authors wish to thank the Natural Sciences and Engineering Research Council of Canada, the Ministry of Intergovernmental and Aboriginal Affairs of New Brunswick, the "Ministère de l'Éducation du Québec" and the Faculty of Graduate Studies and Research of the "Université de Moncton" for financial support to this project. Thanks are also due to the School of Engineering of the "Université de Moncton" for computing facilities.

REFERENCES

[1] Schwabe D., Sharmann A., Some evidence for the existence and a magnitude of a critical Marangoni number for the onset of oscillatory flow in crystal growth melts, J. Crystal Growth 46 (1979) 125–131.

[2] Chun C.H., Marangoni convection in a floating zone under reduced gravity, J. Crystal Growth 48 (1980) 600–610.

[3] Preisser F., Schwabe D., Sharmann A., Steady and oscillatory thermocapillary convection in liquid columns with free cylindrical surface, J. Fluid Mech. 126 (1983) 545–567.

[4] Ostrach S., Kamotani Y., Lai C.L, Oscillatory thermocapillary flows, Phys. Chem. Hydrodynamics 6 (1985) 585–599.

[5] Monti R., Fortezza R., The scientific results of the experiment on oscillatory Marangoni flow performed in Telescience on Texus 23, Micrograv. Q 1 (1991) 163.

[6] Hu W.R., The influence of buoyancy on the oscillatory thermocapillary convection with small Bond number, in: 39th IAF Congress, 1988, Paper No. IAF-88-365.

[7] Kazarinoff N.D., Wilkowski J.S. A numerical study of Marangoni flows in zone-refined silicon crystals, Phys. Fluids A 1 (1989) 625–627.

[8] Clark P.A., Wilcox W.R., Influence of gravity on thermocapillary convection in floating zone melting of Silicon, J. Cryst. Growth 50 (1980) 461.

[9] Xu J.J., Davis S.H., Liquid bridges with thermocapillarities, Phys. Fluids 26 (1983) 2880–2886.

[10] Rybicki A., Florian J.M., Thermocapillary effects in liquid bridges. I. Thermocapillary convection, Phys. Fluids 30 (1987) 1956.

[11] Rybicki A., Florian J.M. Thermocapillary effects in liquid bridges. II. Deformation of the interface and capillary instability, Phys. Fluids 30 (1987) 1973.

[12] Chen G., Roux B. An analytical study of thermocapillary flow and surface deformation in floating zones, Micrograv. Q. 1 (1991) 73.

[13] Napolitano L.G., Viviani A., Marangoni–Stokes flow in axisymmetric bridges, Micrograv. Q. 2 (1992) 179.

[14] Chen H., Saghir M.Z., Three-dimensional Marangoni convection in the asymmetrically heated float zone, Micrograv. Q. 4 (1994) 39.

[15] Bazzi H., Nguyen C.T., Galanis N., Transient behaviors of a $NaNO_3$ float zone operating under high marangoni number condition, in: Proc. 1997 ASME Fluids Engineering Division, Summer Meeting, Vancouver (BC), Canada, 1997, Paper No. FEDSM-3390.

[16] Wilcox W.R., 1991 Floating zone melting of electronic materials in space, Proc. 29th AIAA conf., Paper no. AIAA-91-0507.

[17] Vargas M., Ostrach S., Kamotani Y., Surface tension driven convection in simulated floating zone configuration, Rpt., Case Western Reserve University, 1982.

[18] Kamotani Y., Ostrach S., Vargas M., Oscillatory thermocapillary convection in a simulated floating zone configuration, J. Crystal Growth 66 (1984) 83–90.

[19] Kamotani Y., Lee K.J. Oscillatory thermocapillary flow in a liquid column heated by a ring heater, Phys. Chem. Hydrodynamics 11 (1989) 729–736.

[20] Napolitano L.G., Monti R., Surface driven flows: recent theoretical and experimental results, in: ESA SP 256, 1987, pp. 551–555.

[21] Rupp R., Müller G., Neumann G., Three-dimensional time-dependent modeling of the Marangoni convection in zone melting configuration of GaAs, J. Crystal Growth 97 (1) (1989) 34–41.

[22] Kazarinoff N.D., Wilkowski J.S., Marangoni flows in a cylindrical liquid bridge of silicon, in: Roux B. (Ed.), Numerical Simulation of Oscillatory Convection in Low Pr Fluids, Vieweg, Braunschweig, 1990, pp. 65–73.

[23] Kazarinoff N.D., Wilkowski J.S., Period tripling and subharmonic oscillations in Marangoni flows in a cylindrical liquid bridge, in: Wong R. (Ed.), Proc. Int. Symp. on Asymptotic Comput. Anal., Lecture Notes in Pure and Applied Mathematics, vol. 24, 1990. pp. 265–283.

[24] Levenstam M., Amberg G., Hydrodynamical instabilities of thermocapillary flow in a half-zone, J. Fluid Mech. 297 (1995) 357–372.

[25] Savino R., Monti R., Oscillatory Marangoni convection in cylindrical liquid bridges, Phys. Fluids 8 (11) (1996) 2906–2922.

[26] Schwabe D., Scharmann A., Measurements of the critical Marangoni number of the laminar–oscillatory transition of thermocapillary convection in floating zones, in: Proc. 5th European Symp. on Material and Fluid Sciences in Microgravity, ESA SP-222, 1984, pp. 281–289.

[27] Bazzi H., Étude numérique de l'écoulement transitoire dans une zone flottante. La transition axisymétrique/oscillatoire, Thesis, Department of Mechanical Engineering, Université de Sherbrooke, Québec, Canada, 1999, p. 239.

[28] Patankar S.V., Numerical Heat Transfer and Fluid Flow, Hemisphere, Washington DC, 1980.

[29] Patankar S.V., Innovative Research Inc. microCOMPACT V. 4.0, Reference Manual, Maple Grove, Minnesota (USA), 1996.

[30] Okano Y., Hatano A., Hirata A., Natural and Marangoni convection in a floating zones, J. Chem. Eng. Jpn. 22 (4) (1989) 385–388.

[31] Saghir M.Z., Rosenblat S. 1990. Numerical simulation of tetracosane and cadmium mercury telleride in 1 g and 10^{-3} g environment, in: Proc. 7th European Symp. on Material and Fluid Sciences in Microgravity, ESA SP-295.

[32] Saghir M.Z., Hirata A., Nishizawa S. 1992. Experimental and numerical results of silicone oil column in earth environment, in: Proc 8th Int. Symp. on Space Tech. and Sci., Kagoshima, Japan, pp. 2193–2198.

[33] Chun C.H., Verification of turbulence developing from the oscillatory Marangoni convection in a liquid column, in: Proc. 5th European Symp. on Material and Fluid Sciences in Microgravity, ESA SP-222, 1984, pp. 271–280.

[34] Schwabe D., Scharmann A., Measurement of the critical Marangoni number in a floating zone under reduced gravity, Proc. 4th European Symp. on Material and Fluid Sciences in Microgravity, ESA SP-191, 1983, pp. 213–218.